SUPPORTING INFORMATION (11 figures)

A D-enantiomeric peptide interferes with hetero-association of amyloid-β oligomers and prion protein*

Nadine S. Rösener[1,2], Lothar Gremer[1,2], Elke Reinartz[1], Anna König[1,2], Oleksandr Brener[1,2], Henrike Heise[1,2], Wolfgang Hoyer[1,2], Philipp Neudecker[1,2] and Dieter Willbold[1,2]

From the [1]Institut für Physikalische Biologie, Heinrich-Heine-Universität Düsseldorf, 40225 Düsseldorf, Germany, [2]Institute of Complex Systems, Structural Biochemistry (ICS-6), Forschungszentrum Jülich, 52425 Jülich, Germany

*Running title: *Interference with Aβ-PrP complex formation*

Material included:

References:

1. Orekhov, V. Y., Ibraghimov, I. V., and Billeter, M. (2001) MUNIN: A new approach to multi-dimensional NMR spectra interpretation. *J. Biomol. NMR.* **20**, 49–60

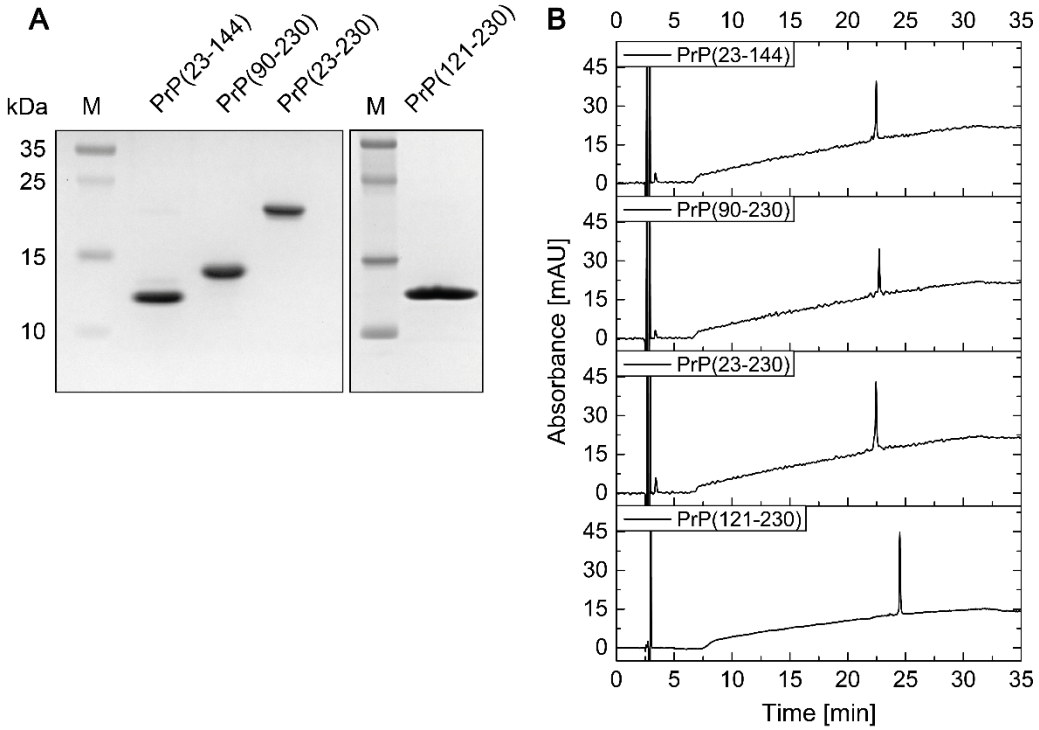

Figure S1: Sample purity of the used huPrP variants (huPrP(23-144), huPrP(90-230), huPrP(23-230) and huPrP(121-230)). 5 µg of each purified huPrP were qualitatively analysed by Tris/Glycine SDS-PAGE (A). RP-HPLC chromatograms show the purity of 1 µM of each huPrP variant (B). The huPrP variants have retention times of about 22 to 24.5 min and were generated in high purity as there are no further peaks visible.

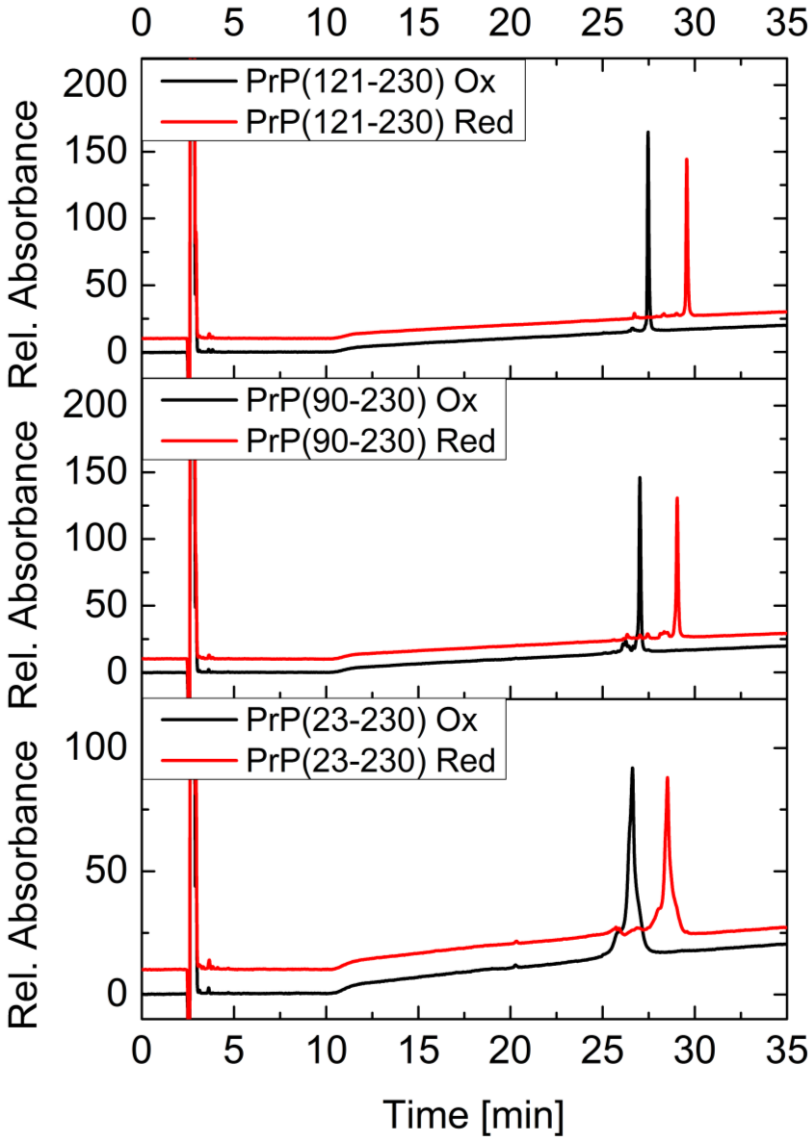

Figure S2: Purified huPrP(23-230), huPrP(90-230) and huPrP(121-230) under study contain a disulfide bond between Cys-179 and Cys-214. The reductive opening of the disulfide bond leads to a characteristic elongation of the retention time in RP-HPLC analyses and verify the exclusive presence of the disulfide bond in purified huPrP(23-230), huPrP(90-230) and huPrP(121-230) and the absence of any reduced fraction in the samples.

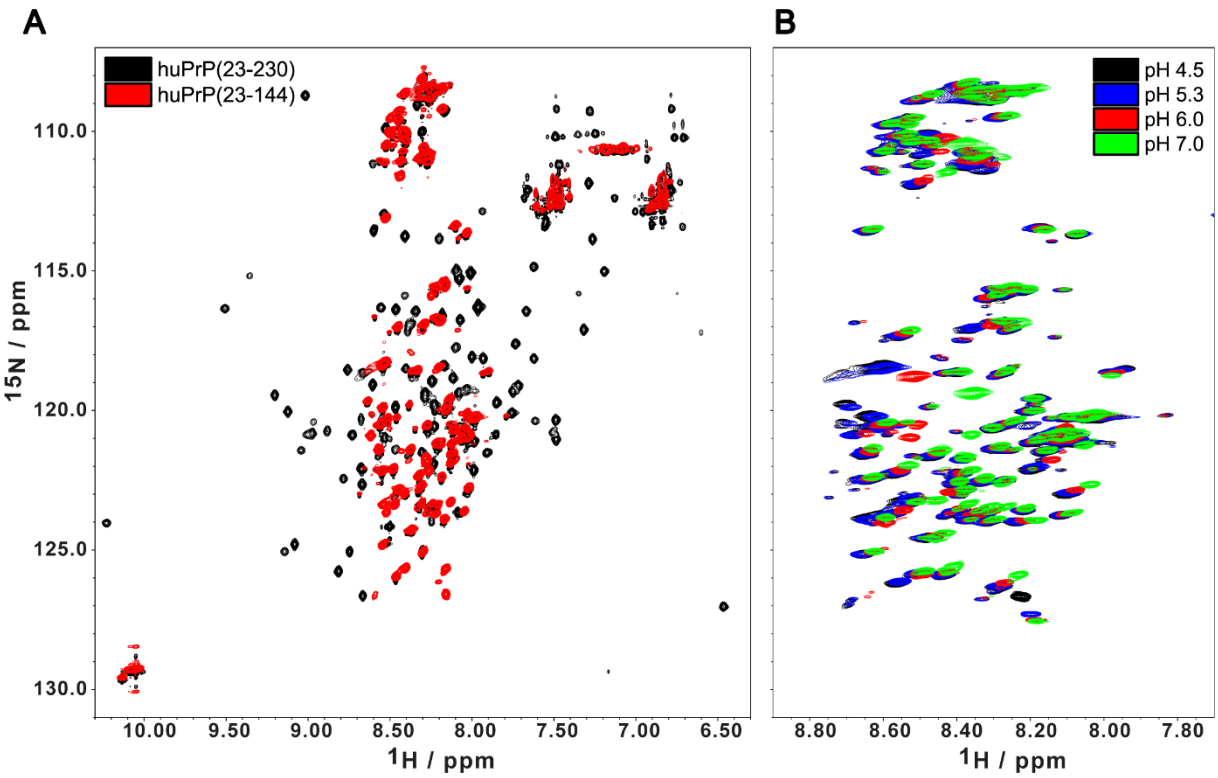

Figure S3: [^{1}H,^{15}N] HSQC NMR spectra of huPrP(23-144) and huPrP(23-230) in solution. (A) Overlay of the [^{1}H,^{15}N] HSQC spectra of 0.2 mM [U-^{15}N] huPrP(23-230) in 10 mM sodium acetate (pH 4.5) in 10 % (v/v) D_2O (black) and of 0.36 mM [U-^{13}C,^{15}N] huPrP(23-144) in 50 mM sodium acetate (pH 4.5) in 10 % (v/v) D_2O (red) recorded at 20.0 °C at 900 MHz and 600 MHz, respectively. Arginine ^{15}Nε side-chain resonances resonating at about 85 ppm are aliased to about 111 ppm in the ^{15}N dimension and show side bands in the ^{1}H dimension due to the limited bandwidth of the WALTZ-16 ^{15}N decoupling during acquisition. Whereas huPrP(23-230) exhibits the well-dispersed backbone amide resonances of the globular C-terminal prion domain, only backbone amide resonances in the random coil region (8.0 ppm < ^{1}H < 8.6 ppm) are visible in the spectrum of the truncation construct huPrP(23-144). (B) Overlay of the backbone amide region of the [^{1}H,^{15}N] HSQC spectra of 0.36 mM [U-^{13}C,^{15}N] huPrP(23-144) in 50 mM sodium acetate (pH 4.5) (black), 0.11 mM [U-^{13}C,^{15}N] huPrP(23-144) in 50 mM sodium acetate (pH 5.3) (blue), 0.28 mM [U-^{13}C,^{15}N] huPrP(23-144) in 50 mM MES (pH 6.0) (red), and 0.30 mM [U-^{13}C,^{15}N] huPrP(23-144) in 50 mM HEPES (pH 7.0) (green) in 10 % (v/v) D_2O recorded at 5.0 °C at 600 MHz, 600 MHz, 800 MHz, and 800 MHz, respectively.

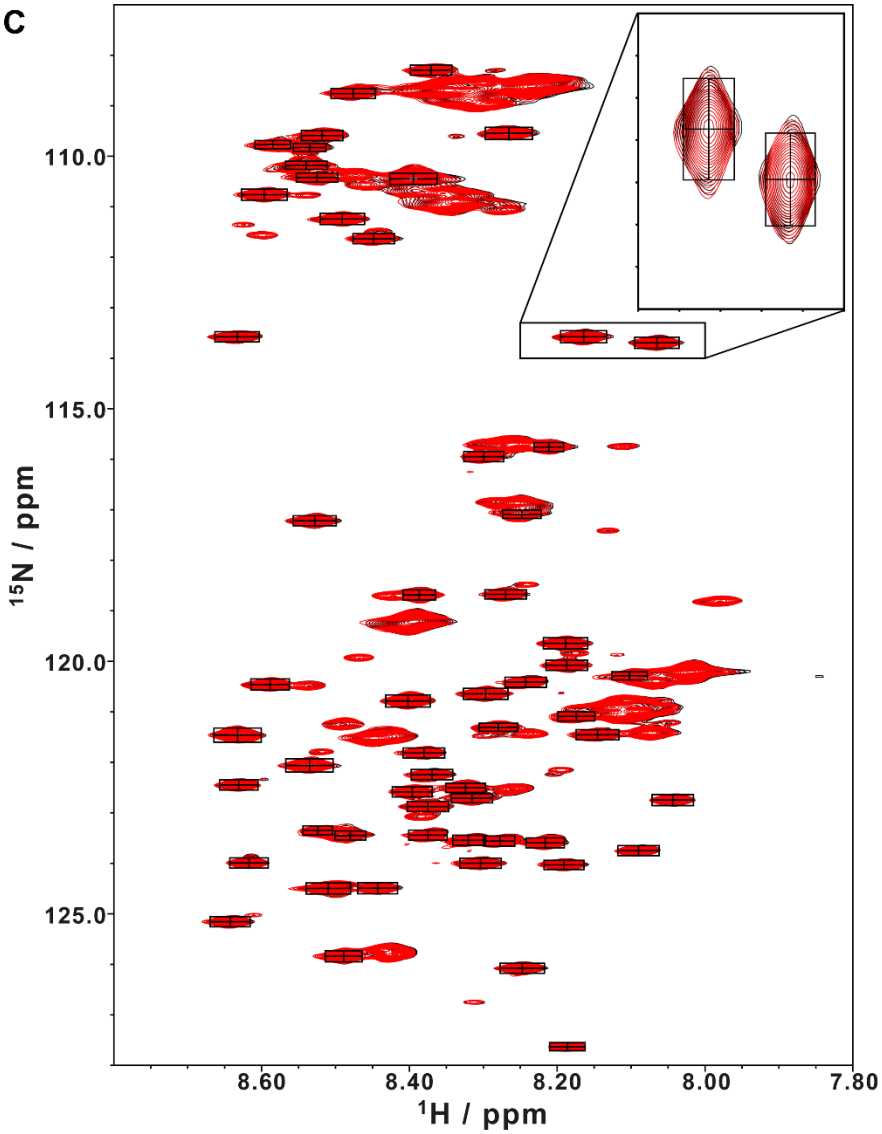

Figure S3 continued: (C) Overlay of the first (time t = 0, black) and the last (t = 55.6 h later, red) [^{1}H,^{15}N] HSQC spectra of a sample of 89 µM [U-^{15}N] huPrP(23-144) with 50 mM Tris-HCl (pH 7.2) in 10 % D_2O in a series of [^{1}H,^{15}N] HSQC spectra recorded at 600 MHz, 5.0 °C. The spectra are so stable over this time period that the contour levels are virtually superimposable, as highlighted by expanding a small region containing two example resonances in the inset. 57 sufficiently well-resolved backbone amide resonances (black rectangular boxes) plus the side-chain indole resonance of Trp99 (which resonates at 10.16 ppm/129.78 ppm in a different region of the spectrum) were selected for quantitative analysis of the peak intensities.

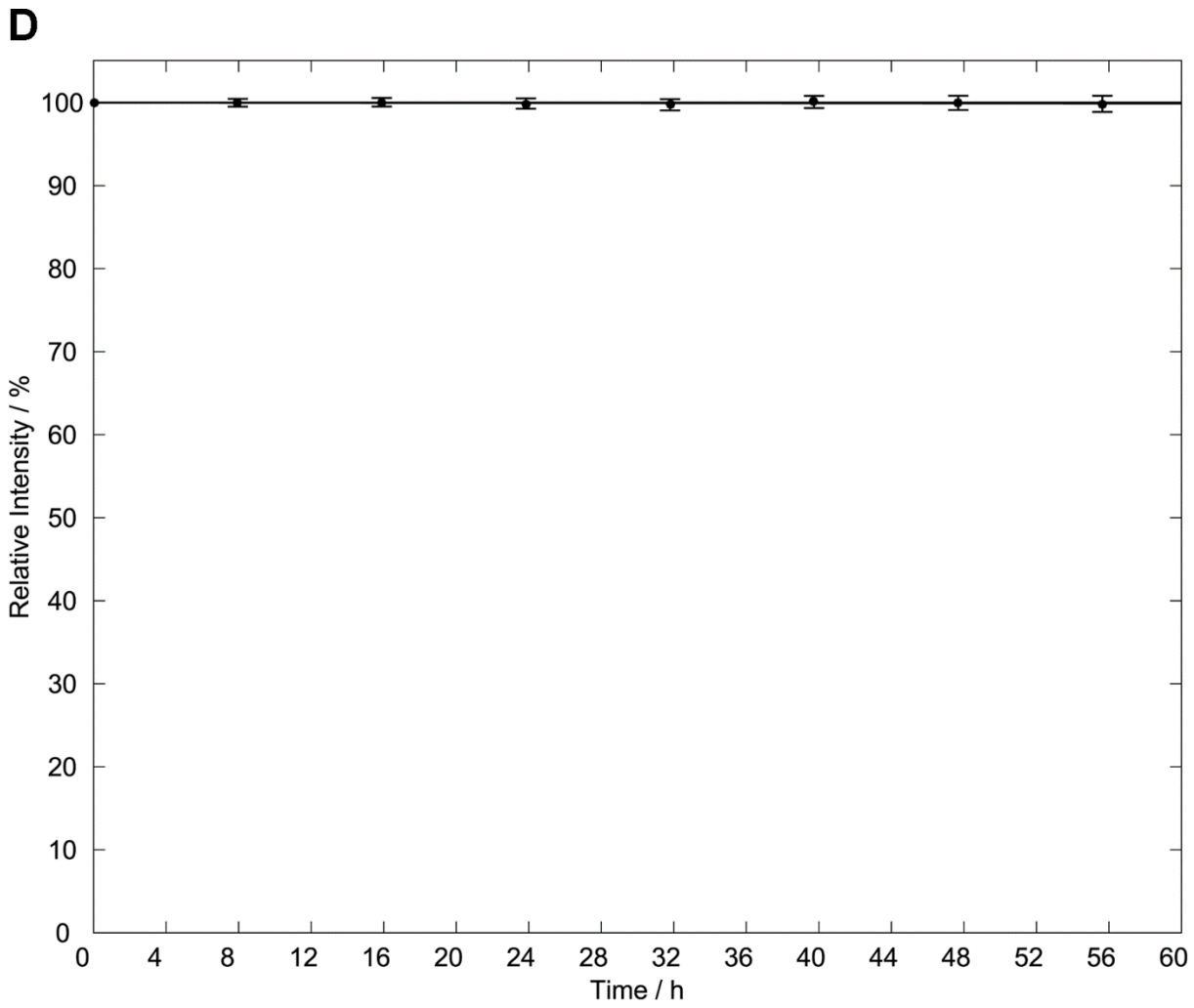

Figure S3 continued: (D) Relative amide resonance intensity of a sample of 89 µM [U-^{15}N] huPrP(23-144) with 50 mM Tris-HCl (pH 7.2) in 10 % D_2O in a series of [^{1}H,^{15}N] HSQC spectra recorded at 600 MHz, 5.0 °C. The intensity of the 58 sufficiently well-resolved amide resonances in the rectangular boxes shown in (C) in the spectrum recorded at time *t* relative to the respective intensity in the first spectrum (time $t = 0$, relative intensity 100 % per definition) was quantified by three-way decomposition using MUNIN: A new approach to multi-dimensional NMR spectra interpretation, *J. Biomol. NMR* **20**, 49-60 (1) and is reported in the form average ± standard deviation. Linear regression yields are relative intensity of 99.992 % - 0.0017 %/h×*t* (solid line), corresponding to an intensity loss of about 0.1 % over the entire observation period of 55.6 h. Because this is within the standard error of the average relative intensity at 55.6 h, we conclude that no statistically significant change in resonance intensity was observed over a period of 55.6 h. The sample had been prepared four days before the start of the first experiment (defined as $t = 0$). Even after four days of storage at 4 °C no significant degradation or nucleation of aggregation had occurred, as evidenced by fact that the [^{1}H,^{15}N] HSQC spectra are free of any degradation products (C) and that no signal loss expected for any sample aggregation was detectable (D).

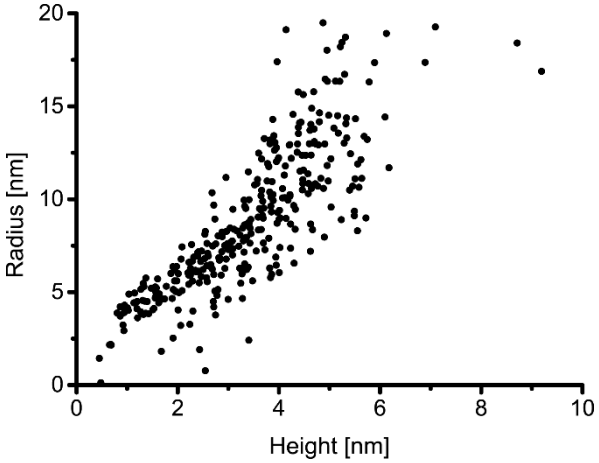

Figure S4: Heights and radii of the generated Aβ(1-42)$_{oligo}$ species as seen by AFM. Aβ(1-42)$_{oligo}$ show a size distribution with heights ranging from 1 nm to 6 nm, very rarely up to 10 nm, and radii up to 20 nm.

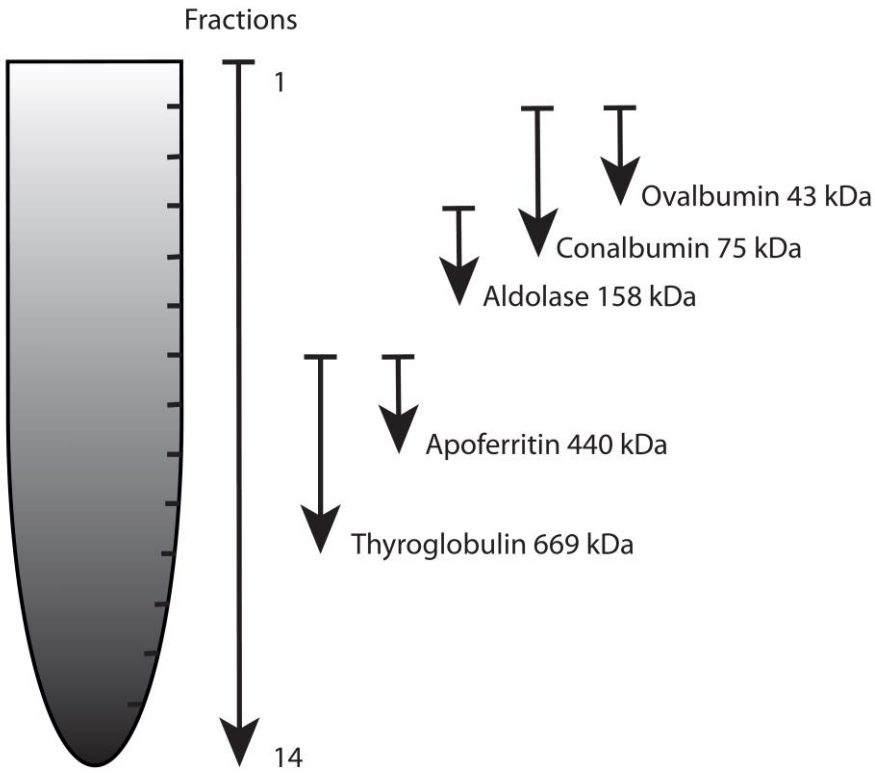

Figure S5: Distribution of standard proteins after sucrose DGC. The protein with the highest molecular mass (thyroglobulin, 669 kDa) was found in fractions 7 to 10.

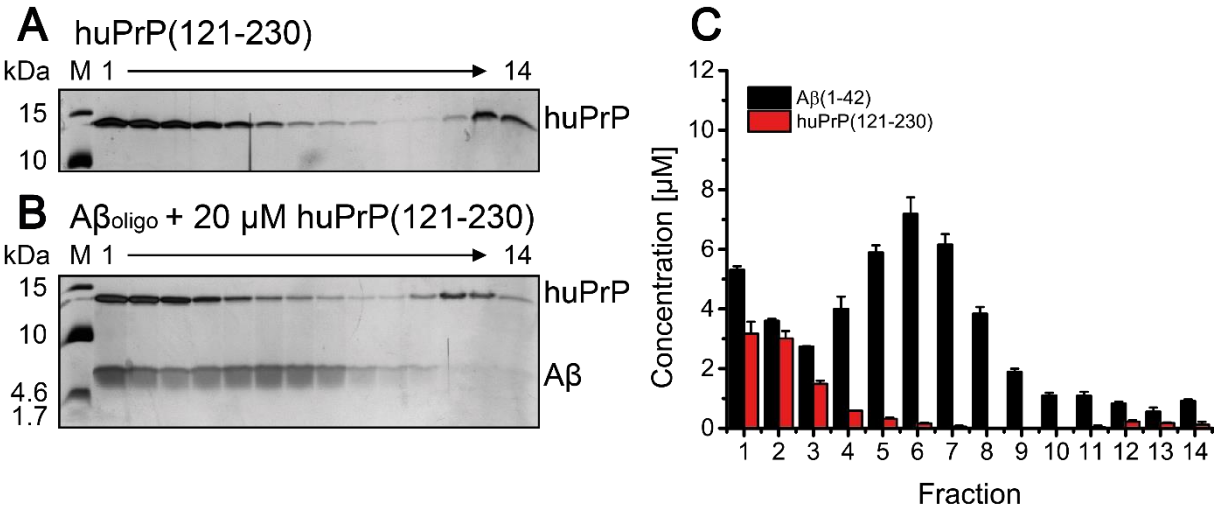

Figure S6: Impaired formation of hetero-assemblies of Aβ(1-42)$_{oligo}$ and huPrP(121-230). (A) Silver-stained Tris/Tricine SDS-PAGE gel after application of 20 µM huPrP(121-230) on a sucrose gradient. (B) Silver-stained Tris/Tricine SDS-PAGE gel after application of 80 µM of pre-incubated Aβ(1-42) with 20 µM huPrP(121-230) on a sucrose gradient and (C) corresponding histogram after RP-HPLC analysis shows the distribution of Aβ(1-42) and huPrP(121-230). huPrP(121-230) was found in fractions 1 to 6 for both the control (A) and in presence of Aβ(1-42)$_{oligo}$ (B). Just very low concentrations below 0.2 µM of huPrP(121-230) were detected in the bottom gradient fractions 11 to 14 as confirmed by RP-HPLC (C). The majority of Aβ(1-42) was observed in fractions 1 to 8 showing a characteristic distribution of Aβ(1-42)$_{oligo}$ in fractions 4 to 8. Just low concentrations of Aβ were found in fractions 11 to 14. Thus, Aβ(1-42)$_{oligo}$ and huPrP(121-230) do not form high molecular weight hetero-assemblies. Experiments are done in replicates of n = 3 (C) ± SD.

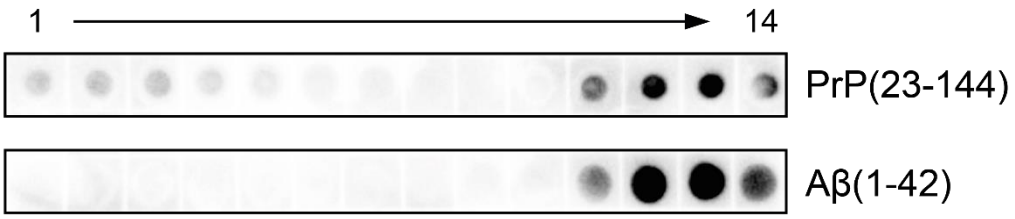

Figure S7: Distribution of Aβ(1-42) and huPrP(23-144) in a sucrose gradient after incubation of 80 µM Aβ(1-42)$_{oligo}$ with 40 µM huPrP(23-144) by immune dot blot. Qualitative analysis was performed by an immune dot blot assay of the DGC fractions with prion antibody Saf32 or Aß42 binding IgG IC16. Aβ(1-42) is entirely bound to huPrP(23-144) and thereby detected in fractions 11 to 14. huPrP(23-144) was used in excess and is found in fractions 11 to 14 (complexes) as well as in fractions 1 to 4 in its soluble non-aggregated state.

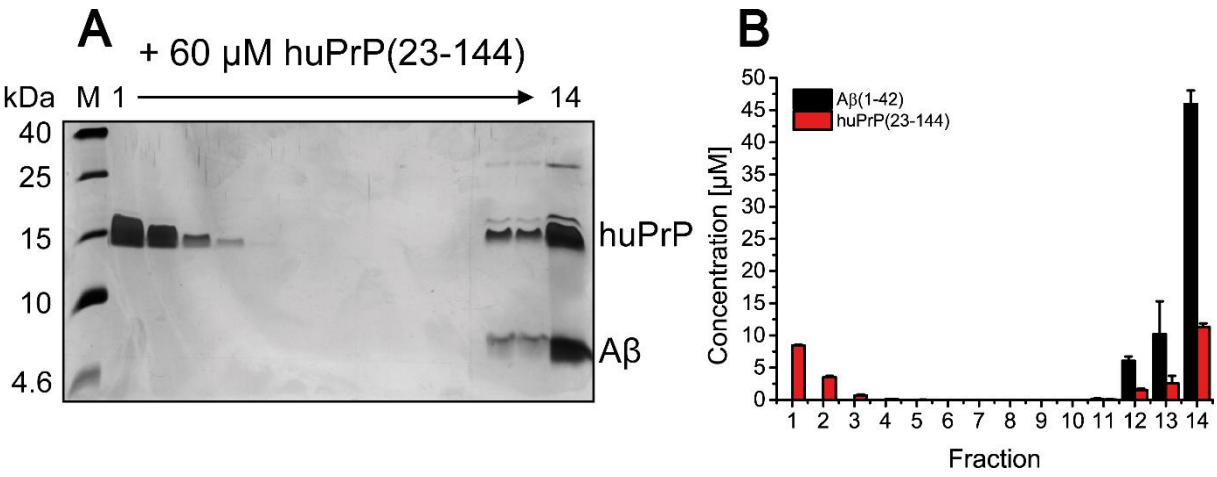

Figure S8: Distribution of Aβ(1-42) and huPrP(23-144) in a sucrose gradient after incubation of $Aβ(1-42)_{oligo}$ with 60 µM huPrP(23-144). (A) Silver-stained Tris/Tricine SDS-PAGE gel after application of 80 µM of pre-incubated Aβ(1-42) with 60 µM huPrP(23-144) on a sucrose gradient and (B) corresponding histogram after RP-HPLC analysis shows the distribution of Aβ(1-42) and huPrP(23-144). Aβ(1-42) is entirely bound to huPrP(23-144) and thereby detected in fractions 12 to 14. huPrP(23-144) was used in excess and is found in fraction 12 to 14 (complexes) as well as in fractions 1 to 4 in its soluble non-aggregated state. Experiments are done in replicates of n = 3 (B) ± SD.

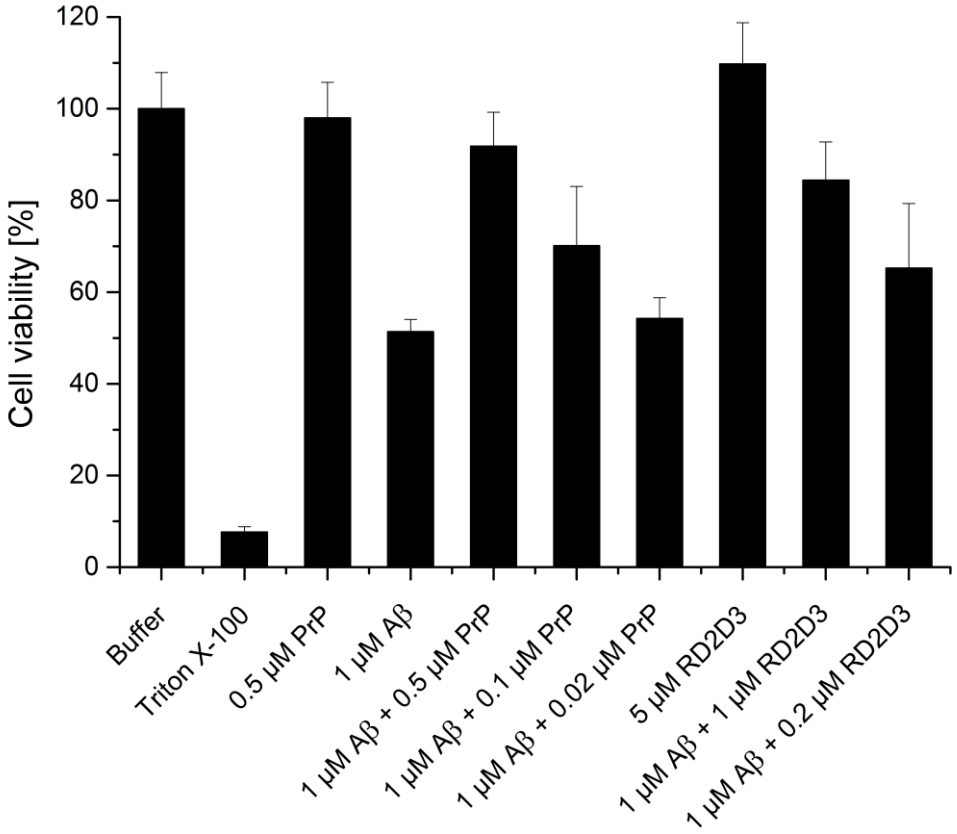

Figure S9: Anchorless huPrP(23-144) or RD2D3 rescue the negative impact of Aβ(1-42)$_{oligo}$ on cell viability in PC-12 cells. Cell viability was assessed by MTT assay after incubation of PC-12 cells with 1 µM Aβ(1-42)$_{oligo}$ alone or either after mixing and further incubation of Aβ(1-42)$_{oligo}$ with 0.02, 0.1 or 0.5 µM huPrP(23-144) or with 0.2, or 1 µM RD2D3, respectively. Data confirms the efficacy of anchorless huPrP(23-144) or RD2D3 to rescue the cell viability in a concentration-dependent manner after incubation with Aβ(1-42)$_{oligo}$ compared to Aβ(1-42)$_{oligo}$ alone. Cells treated with 0.125 % Triton X-100 were used as a positive control. Results were normalised to cells treated with buffer only. Values are means ± SD of 15 replicates.

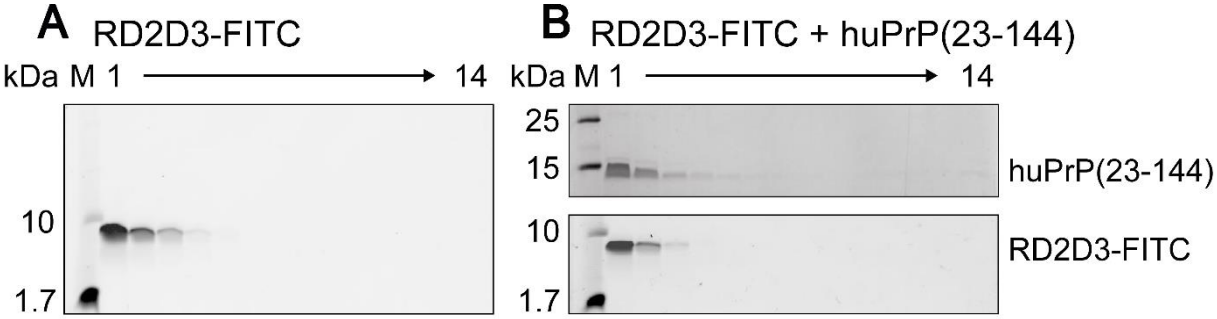

Figure S10: Distribution of 40 µM RD2D3-FITC alone (A) and of 20 µM RD2D3-FITC with 10 µM huPrP(23-144) (B) after sucrose DGC. RD2D3-FITC alone was detected in fractions 1 to 4 after fluorescence detection of a Tris/Tricine SDS-PAGE gel and is therefore present in a soluble and not aggregated state (A). RD2D3-FITC and huPrP(23-144) were incubated for 30 min before analysis by sucrose DGC and were both found in fractions 1 to 4 in a Tris/Tricine SDS-PAGE gel (B). The Tris/Tricine SDS-PAGE gel on the top was stained with silver and the gel on the bottom shows the same gel after fluorescence detection of RD2D3-FITC and before silver staining. As there are no bands visible in fractions 11 to 14, huPrP(23-144) and RD2D3-FITC do not form high molecular weight aggregates.

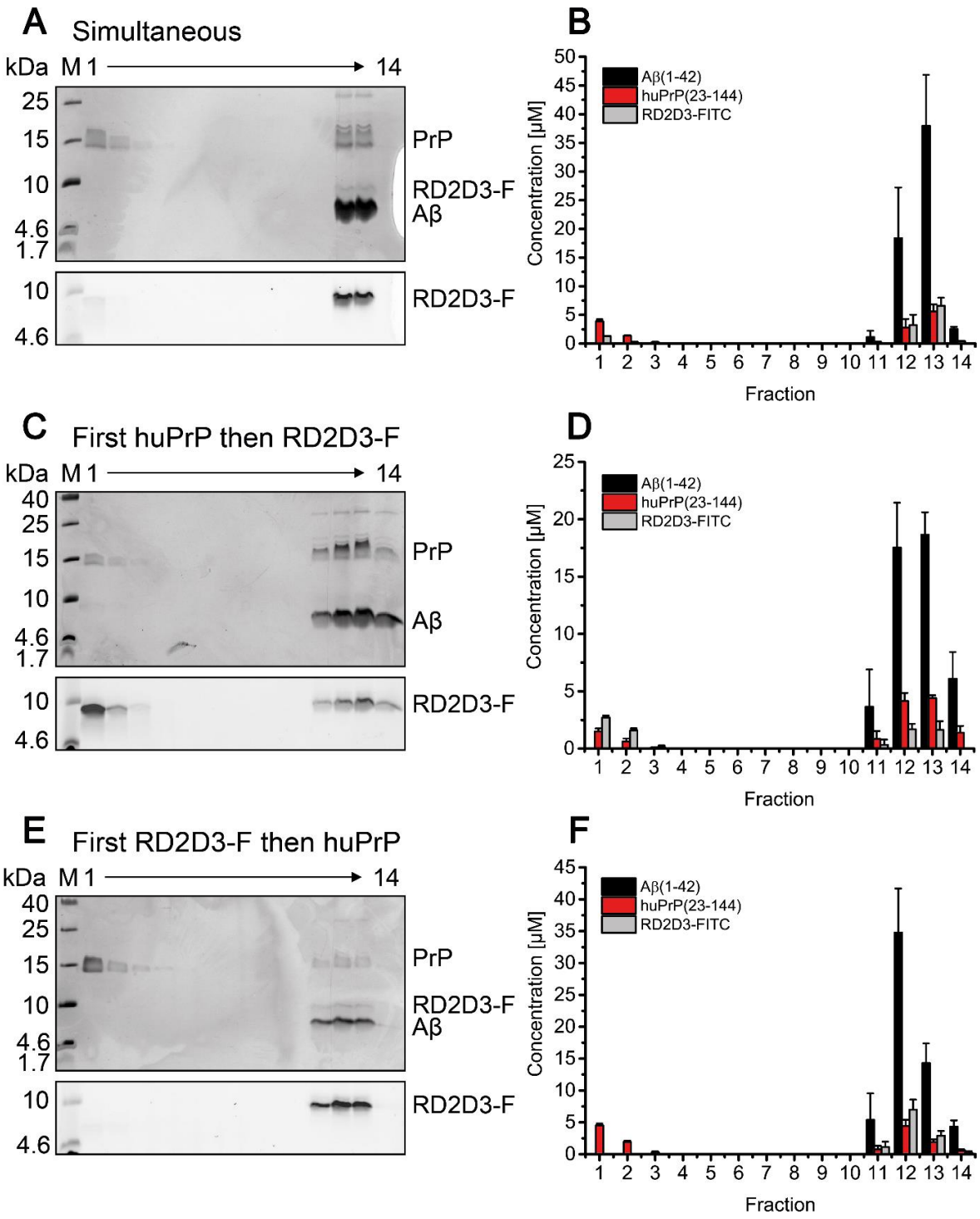

Figure S11: Interference of the Aβ(1-42)$_{oligo}$-huPrP(23-144) interaction by RD2D3-FITC. Distribution of 80 µM Aβ(1-42), 40 µM huPrP(23-144), and 20 µM RD2D3-FITC, after sucrose DGC for different orders of RD2D3-FITC and huPrP(23-144) addition. (A, C and E) Aβ(1-42) and huPrP(23-144) distributions are shown in silver-stained Tris/Tricine SDS-PAGE gels and the distribution of RD2D3-FITC after fluorescence detection on the same gels. (B, D and F) Quantification by RP-HPLC of each component. huPrP(23-144) and RD2D3-FITC were either (A, B) simultaneously added to Aβ(1-42)$_{oligo}$, (C, D) huPrP(23-144) was pre-incubated with Aβ before RD2D3-FITC addition, or (E, F) RD2D3-FITC was pre-incubated with Aβ before huPrP(23-144) addition. Dependent on the order of application of RD2D3-FITC or huPrP(23-144) to the sample, the distributions of huPrP(23-144) and RD2D3-FITC change. Experiments are done in replicates of n = 3 ± SD for all orders of application of RD2D3-FITC or huPrP(23-144) to the sample.